

Validation of $\Delta H(M, \Delta M)$ -technique for identification of switching field distributions in the presence of thermal relaxation

O. Hovorka, R. F. L. Evans, R. W. Chantrell, Y. Liu, K. A. Dahmen et al.

Citation: *J. Appl. Phys.* **108**, 123901 (2010); doi: 10.1063/1.3517823

View online: <http://dx.doi.org/10.1063/1.3517823>

View Table of Contents: <http://jap.aip.org/resource/1/JAPIAU/v108/i12>

Published by the [American Institute of Physics](#).

Related Articles

Dynamics and collective state of ordered magnetic nanoparticles in mesoporous systems

J. Appl. Phys. **112**, 094309 (2012)

Oscillation frequency of magnetic vortex induced by spin-polarized current in a confined nanocontact structure

J. Appl. Phys. **112**, 093905 (2012)

Coercivity enhancement in Pr_{9.5}Fe₈₃Zr₂B_{5.5} magnetic nanomaterials

J. Appl. Phys. **112**, 073924 (2012)

Amorphous Slater-Pauling like behaviour in magnetic nanoparticles alloys synthesized in liquids

J. Appl. Phys. **112**, 063910 (2012)

On the influence of nanometer-thin antiferromagnetic surface layer on ferromagnetic CrO₂

J. Appl. Phys. **112**, 053921 (2012)

Additional information on J. Appl. Phys.

Journal Homepage: <http://jap.aip.org/>

Journal Information: http://jap.aip.org/about/about_the_journal

Top downloads: http://jap.aip.org/features/most_downloaded

Information for Authors: <http://jap.aip.org/authors>

ADVERTISEMENT



Goodfellow
metals • ceramics • polymers • composites
70,000 products
450 different materials
small quantities fast

www.goodfellowusa.com

Validation of $\Delta H(M, \Delta M)$ -technique for identification of switching field distributions in the presence of thermal relaxation

O. Hovorka,^{1,a)} R. F. L. Evans,² R. W. Chantrell,² Y. Liu,³ K. A. Dahmen,⁴ and A. Berger¹

¹*CIC nanoGUNE Consolider, Donostia-San Sebastián 20018, Spain*

²*Department of Physics, The University of York, Heslington, York YO10 5DD, United Kingdom*

³*Center for Complex Network Research at Northeastern University, Boston, Massachusetts 02115, USA*

⁴*Department of Physics, University of Illinois at Urbana Champaign, Urbana, Illinois 61801, USA*

(Received 7 May 2010; accepted 24 October 2010; published online 17 December 2010)

The potential of hysteresis loop-based methods for the characterization of granular magnetic materials is investigated in the presence of thermal relaxation effects. Specifically, we study the reliability of the $\Delta H(M, \Delta M)$ -method to recover the intrinsic switching field distribution in the presence of thermal relaxation. As input data, we use the computational results obtained from kinetic Monte Carlo simulations of interacting Stoner–Wohlfarth particle arrays including the anisotropy field and grain size distributions, and then analyze them using the hysteron-based $\Delta H(M, \Delta M)$ -method to identify the accuracy limits of this methodology. It is found that the accuracy of the $\Delta H(M, \Delta M)$ -method is not substantially changed by the presence of thermal relaxation. © 2010 American Institute of Physics. [doi:10.1063/1.3517823]

I. INTRODUCTION

Magnetic hysteresis in interacting nanoparticle arrays is governed by the complex interplay between magnetic interactions and various sources of inhomogeneity present in the material. The behavior is complicated even further by the presence of thermal fluctuations, which are hard to separate from nonthermal effects. Thermal excitation of magnetic moment is particularly relevant in magnetic recording where it is a primary factor responsible for a deteriorating stability of information, and puts limits on the achievable density of a bit pattern.^{1,2} In addition, it leads to a field rate dependence of the hysteresis³ and complicates the interpretation of hysteresis loop based identification of intrinsic materials characteristics. The issue of magnetic characterization in the presence of thermal relaxation will be addressed in the present paper.

An important characteristic of granular magnetic materials, such as perpendicular recording media, is the intrinsic switching field distribution (SFD).^{1,2} It is the probability distribution for switching fields of individual material particles in the interaction-free case and carries information about the anisotropy and volumetric distributions of particles. This characteristic is important because it is one key factor determining the quality of perpendicular recording media. The presence of interactions and thermal relaxation results in shifted switching fields of particles and the SFD can no longer be extracted from hysteresis loops directly without using modeling assumptions. Among the most common methods for extracting the SFD from the laboratory time scale measurements, which are typically on the order of seconds, were the FORC method similar to the Preisach model,^{4,5} van de Veerdonk's method based on the assumption of a constant demagnetization factor,⁶ the method by Tagawa and Nakamura,⁷ and the $\Delta H(M, \Delta M)$ -method.^{8,9} These

methods are based on variable degrees of approximation but their common feature is that they essentially ignore the separate role of thermal relaxation effects. It is then unclear how accurate the methods are and, equally important, how they relate to the fast sub-nanosecond time-scale relevant for write processes in hard disk drives.^{10,11}

To understand this issue we study the most commonly used and advanced $\Delta H(M, \Delta M)$ -method. The method is based on the interacting hysteron model of perpendicular recording media. It was originally developed assuming the mean-field approximation^{8,9} and recently extended beyond the mean-field picture as well.^{12,13} We study the accuracy of both variations in the technique by using as an input the data computed from the more general computational Stoner–Wohlfarth model (SW) with exchange and dipolar interparticle interactions,¹⁴ which was set-up to mimic perpendicular recording materials. Thermal relaxation is accounted for in the model via an Arrhenius–Neél-type process describing the hopping over the distribution of energy barriers, which sets the characteristic thermal relaxation timescale and governs the dependence of hysteresis loops from the speed of the external field variation. Analysis of hysteresis loops computed from the SW-model for different exchange and dipolar strengths shows that the mean-field $\Delta H(M, \Delta M)$ -method is capable of identifying the SFD accurately for all rates considered as long as the exchange and dipolar interactions are of a comparable strength, which is consistent with the previous results for nonthermal models.¹⁵ On the other hand, the extended $\Delta H(M, \Delta M)$ -method, which will be called the 'reference function $\Delta H(M, \Delta M)$ -method', allows accurate identification in a much broader interaction range when intergranular interactions are not too strong in comparison to the average anisotropy in the system, i.e., the materials parameter range relevant for perpendicular magnetic recording media. Stronger interparticle interactions lead to the possibility of noncollinear magnetization states and reversible magneti-

^{a)}Electronic mail: o.hovorka@nanogune.eu.

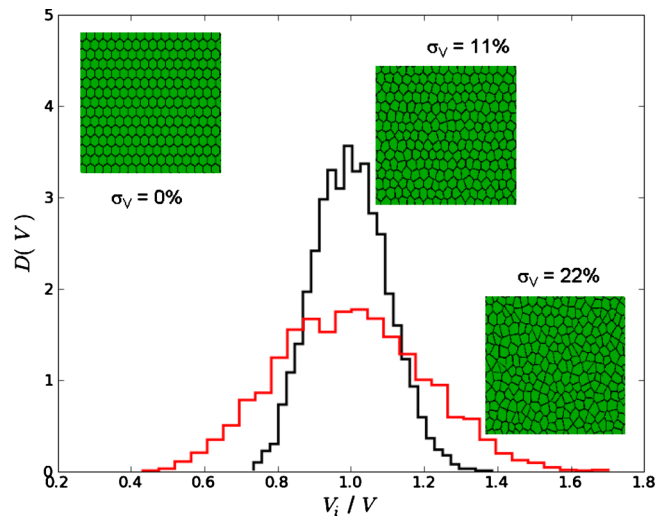


FIG. 1. (Color online) Three different grain size distributions considered in the study. Shown are also histograms of grain size distributions.

zation processes, which cannot be captured by any of the above mentioned characterization methodologies based on hysterons because they do not include the possibility of reversible magnetization changes.

II. KINETIC MONTE-CARLO MODEL

The model has been introduced in general terms in Ref. 14. To model perpendicular recording materials, we assume a planar assembly of N SW particles, $i=1, \dots, N$, having volumes V_i and saturation magnetization M_S . The magnetization of every particle normalized by M_S is described by a dimensionless unit vector \vec{m}_i which is free to rotate. A distribution of volumes, $D(V)$, is generated using Voronoi tessellations with the uniform case corresponding to a regular hexagonal lattice with spacing a . The mean of $D(V)$ will be denoted by V and the standard deviation by σ_V (Fig. 1). The anisotropy axes of the particles are oriented perpendicular to the plane, i.e., $\vec{K}_i = K_i \hat{z}$, and aligned with the external field \vec{H}_a . Because of this orientation, particles in the interaction-free case lack any reversible magnetization component. Anisotropy constants K_i vary randomly from particle to particle according to the lognormal probability distribution. Defining the anisotropy fields as $H_{K,i} = 2 K_i / M_S$ (CGS units) defines the lognormal anisotropy field distribution $D(H_K)$. The mean anisotropy field will be denoted as H_K and the standard deviation by σ_K (see also Sec. III). The interparticle exchange interaction is quantified by a locally varying exchange field $\vec{H}_{EX,i} = z^{-1} H_{EX} \sum_j f_{ij} \vec{m}_j$. The exchange field is considered to be determined by the contact area between grains, which leads to f_{ij} as the weighting function between grains i and j . This factor is determined by the Voronoi construction. The macroscopic exchange field parameter H_{EX} is equal to the mean exchange field at saturation (z is the local coordination number associated with a grain i). Dipolar interaction fields acting on individual particles defined as $\vec{H}_{DP,i} = a^{-3} V_i M_S \sum_j (\vec{m}_j r_{ij}^{-3} - \vec{r}_{ij} (\vec{m}_j \cdot \vec{r}_{ij}) r_{ij}^{-5})$, with r_{ij} the distance between the particles i and j normalized by a , are long-range and for the sake of efficiency are truncated at a cutoff distance $r_{ij} < R$. The long-

range part is included via an effective mean-field approximation. Calculations show that a truncation range of $R=8$ diameters is sufficiently large to provide an accurate calculation of the magnetostatic field.

The total effective field acting on a particle i is given by the following:

$$\vec{H}_i = H_a \hat{z} + \vec{H}_{EX,i} + \vec{H}_{DP,i}, \quad (1)$$

and the associated free energy of the SW particle i is:

$$E_i = E_{0,i} \left(\frac{1}{2} \sin^2 \alpha_i - \frac{\vec{H}_i \cdot \vec{m}_i}{H_{K,i}} \right). \quad (2)$$

Here the first term is the anisotropy energy with $\cos \alpha_i = \hat{z} \cdot \vec{m}_i$, the second term is the total effective field energy, and the energy constant is $E_{0,i} = M_S V_i H_{K,i}$. For external fields less than the critical field defined by the SW astroid (the important case for thermally activated reversal),¹⁶ minimization of Eq. (2) gives two stable moment orientations along or against the anisotropy axis, respectively, with $\cos \alpha_i > 0$ or $\cos \alpha_i < 0$, which will be referred to as (+) or (-) states. Thermal switching between the stable states of a particle i is governed by the Arrhenius–Neél relaxation law, as follows:

$$w_i^\pm = f_0 \exp(-E_{B,i}^\pm / k_B T), \quad (3)$$

where we use here the frequency factor $f_0 = 10^{10} \text{ s}^{-1}$. k_B is the Boltzmann constant, T is the temperature, and w_i^+ and w_i^- are the transition rates for switching from (+) to (-) over the effective field-dependent energy barrier $E_{B,i}^+$, and from (-) to (+) over the energy barrier $E_{B,i}^-$, respectively. $E_{B,i}^\pm$ are computed from local extrema of the energy (2).

The evolution of the magnetic state is calculated as follows. The external field H_a is set and held constant for a certain time, essentially modeling a stepped field experiment. At each external field value the effective fields \vec{H}_i acting on every particle are first evaluated, following which the energy barriers $E_{B,i}^\pm$ and the transition rates w_i^\pm are determined from Eqs. (2) and (3). Particles are then picked at random and switched to follow the time evolution of their respective transition probability, as follows:

$$P_i(t_m) = P_i^0 \exp(-t_m / \tau_i) + w_i^+ \tau_i [1 - \exp(-t_m / \tau_i)], \quad (4)$$

which was obtained by solving the corresponding master equation.¹⁴ In (4), P_i^0 is the initial probability of finding a particle i in the (-) state and $P_i(t_m)$ is the probability of preserving that state after the characteristic measurement time t_m . τ_i is the particle relaxation time $\tau_i^{-1} = w_+ + w_-$. The first term in Eq. (4) describes, in the particle's state space, a distance from the initial state while the second term describes the approach to the equilibrium. In subsequent steps within the iteration at H_a all particles are picked one after another and flipped according to their respective realizations of Eq. (4), with effective fields and transition rates recalculated after each flipping process of a particle. To achieve good statistics for a reliable representation of the probabilities P_i^0 and P_i this entire procedure is repeated q times. We found that for a perpendicular anisotropy system of 160×160 particles at $T=300 \text{ K}$, considered in the present work, setting $q=5$ did not produce results different in any signifi-

cant way than for $q \gg 5$ if H_{EX} values were less than 12 kOe. However, for stronger exchange interactions large values of q are anticipated for algorithm to converge to a metastable state. Finally, to complete the iteration at the field H_a , the magnetization M of the system is calculated by averaging over the projections of particle moments onto the \hat{z} -axis. Then H_a is incremented by δH_a and the entire process repeats. In this way, the model allows the computation of hysteresis loops M vs. H_a for different exchange and dipolar interactions and for different characteristic times t_m . The time t_m is the parameter determining the relative importance of thermal relaxation. The external field sweep rate will be defined by a ratio $r = \delta H_a / t_m$. Finally we mention that because the present implementation of the model does not include truly dynamical effects of the particle switching, such as precession of particle moments, it is naturally not expected to fully capture the physics of magnetization reversal at very short sub-nanosecond time scales on the order $1/f_0$ or less. This puts an upper limit on the frequencies, which are expected to be realistically described by the model.

III. INTRINSIC SFD $D(H_S)$

In general terms, the intrinsic SFD is defined as the probability of particle i having a switching field $H_{S,i}$, in the interaction free case. Knowledge of the switching fields of particles can provide information about the distributions of anisotropy $D(H_K)$ and volumes of particles, for example, which is important for the design and optimization of perpendicular recording materials. The aim is to extract the $D(H_S)$ from hysteresis loops.¹

The stability analysis of Eq. (2) reveals that the field $H_{S,i}$ at which a particle switches irreversibly between its (+) and (−) states in the nonthermal case is defined by the SW astroid and equals to the following:¹⁶

$$H_{S,i} = H_{K,i} (\cos^{2/3} \alpha_i + \sin^{2/3} \alpha_i)^{-3/2}. \quad (5)$$

The intrinsic SFD $D(H_S)$ is defined as probability for $H_{S,i}$ if all interactions in the particle system were absent. Thus in the SW particle system $D(H_S)$ is generally directly related to both $D(H_K)$ and the distribution of α_i . In the present work, the situation is simplified by the assumption of an external field-anisotropy axis alignment, i.e., $\alpha_i = 0$. Both $D(H_S)$ and $D(H_K)$ then coincide if thermal relaxation effects are absent. In what follows, the experimentally often observed lognormal distribution $D(H_K)$ will be assumed and, as a result, the SFD for the relaxation-free case can be defined as follows:

$$D(H_S) \equiv D(H_K) = (\sqrt{2\pi}\tilde{\sigma}_K H_K)^{-1} \times \exp[-(\ln H_K - \tilde{\mu}_K)^2 / 2\tilde{\sigma}_K^2]. \quad (6)$$

In Eq. (6), $\tilde{\mu}_K$ and $\tilde{\sigma}_K$ are the mean and the standard deviation of a random variable $\ln(H_{K,i})$. We note that the distribution Eq. (6) can also be uniquely defined in terms of the standard deviation σ_K related to $\tilde{\mu}_K$ and $\tilde{\sigma}_K$ as $\sigma_K^2 = (\exp(\tilde{\sigma}_K^2) - 1) \times \exp(2\tilde{\mu}_K + \tilde{\sigma}_K^2)$, and the skewness factor $\gamma(\tilde{\sigma}_K) = (\exp(\tilde{\sigma}_K^2) + 2) \sqrt{\exp(\tilde{\sigma}_K^2) - 1}$ quantifying asymmetry of $D(H_S) \equiv D(H_K)$.

If thermal relaxation effects are present the switching of particles aided by thermal excitations will occur at lower

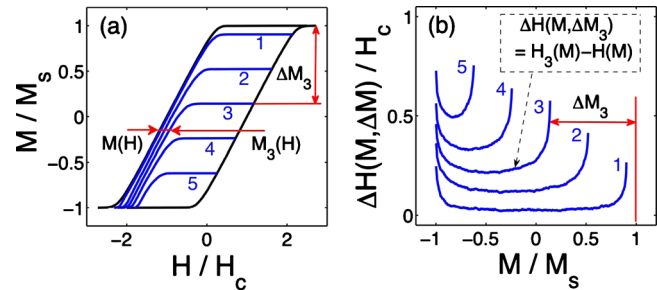


FIG. 2. (Color online) (a) Major hysteresis loop and recoil curves at distances $\Delta M_i, i=1, \dots, 5$, from saturation. (b) $\Delta H(M, \Delta M_i)$ are the field differences between the recoil curves and the major loop, i.e., $H_3(M) - H(M)$. The axes are normalized with respect to the saturation magnetization M_s and the coercive field H_c .

fields $H_{S,i} < H_{K,i}$ hereby causing nontrivial modifications to $D(H_S)$. Assuming the grain volumes and the temperature to be fixed, the relative importance of thermal effects can be tuned in the model by choosing the characteristic measurement time scale t_m , i.e., the external field rate $r = \delta H_a / t_m$ defined in Sec. II. According to Eq. (4), the effect of thermal relaxation becomes irrelevant only for short times $t_m \ll \tau$, i.e., for high r , hereby leading to coincidence between $D(H_S)$ and $D(H_K)$, but needs to be considered otherwise.

The dependence of $D(H_S)$ on r can be obtained from hysteresis loops computed in the model when all interactions are turned off. Then in the case studied here of aligned easy axes collinear with the applied field, the hysteresis loop is a superposition of reversals of individual particles occurring when the evolving external field H_a matches their respective fields $H_{S,i}$. Consequently $D(H_S)$ can be obtained simply by differentiation of the major loop with respect to the external field from this noninteracting case. This is obviously not the case if interactions are included and the switching fields of particles are dependent on the magnetic state of the entire system. In what follows, the standard deviation of the intrinsic $D(H_S)$ obtained at a given r by differentiating the hysteresis loop of the noninteracting system will be denoted as $\sigma = \sigma(r)$. For high r , σ approaches σ_K defined by Eq. (6). Thus this relationship in principle allows to relate the SFDs at different levels of thermal relaxation and extrapolation to the nonthermal case when $D(H_S) = D(H_K)$. The question addressed here is whether the “intrinsic” σ , i.e., corresponding to the noninteracting case, can in general be obtained from hysteresis loops obtained from interacting particle assemblies.

IV. $\Delta H(M, \Delta M)$ -METHOD FOR IDENTIFICATION OF $D(H_S)$

The purpose of the $\Delta H(M, \Delta M)$ -method is the identification of the intrinsic switching field distributions from hysteresis loops. The method measures the field-differences between the recoil curves at a certain distance ΔM away from saturation (Fig. 2). It has been developed based on the nonthermal case assuming that particles can be described as hysterons (i.e., free of any reversible magnetization switching) with well defined symmetric up and down switching thresholds $\pm H_{S,i}$. Here, we briefly describe two different imple-

mentations of this method, representing different levels of sophistication in terms of the data analysis schemes. In the next Sec. V, the methods will be tested based on the hysteresis data computed from the SW-model in the presence of thermal relaxation.

A. Mean-field method

In the mean-field approximation which can be derived systematically from the nonthermal interacting hysteron model with exchange and dipolar interactions,^{8,9,12} this formulation allows to analytically calculate a major loop and recoil curves and express the field-differences as follows:

$$\Delta H(M, \Delta M) = I^{-1}[(1 - M)/2] - I^{-1}[(1 - M - \Delta M)/2], \quad (7)$$

where $I^{-1}(y)$ is the inverse of the integral $y = I(x) = \int_{-\infty}^x D(H_S) dH_S$. The mean-field formula (7) is independent of interactions and includes only parameters of the SFD. Using Eq. (6) for SFD and Eq. (7), the field-differences can be expressed as follows:

$$\begin{aligned} \Delta H(M, \Delta M) = \sigma F(M, \Delta M; \tilde{\sigma}) = \sigma \{ & \exp[-\sqrt{2}\tilde{\sigma}erf^{-1}(M)] \\ & - \exp[-\sqrt{2}\tilde{\sigma}erf^{-1}(M + \Delta M)] \} \\ & \times [\exp(2\tilde{\sigma}^2) - \exp(\tilde{\sigma}^2)]^{-1/2}, \quad (8) \end{aligned}$$

where σ is the standard deviation of $D(H_S)$ and $\tilde{\sigma}$ is related to the skewness factor $\gamma(\tilde{\sigma})$ as discussed in the previous section. Formulation of the method in terms of the complementary variables $\tilde{\sigma}$ and $\tilde{\mu}$ can be found in.¹⁷ Thus according to expression (8), the $\Delta H(M, \Delta M)$ data set is a product of σ of the SFD and a function F which includes detailed information about the shape of the SFD. We note, that the structure of Eq. (8) taking a form of a product of σ and σ -independent function F , turns out to be a general feature of the interacting hysteron model and holds for any well-behaved form of the SFD.¹⁵

Generally, the mean-field $\Delta H(M, \Delta M)$ -method is applied by fitting formula (8) to measurement data and identifying σ as a fit parameter σ_{fit} . The quality of fitting is quantified by the multiple correlation coefficient R^2 , which essentially indicates the applicability of the mean-field hysteron model to the input data entering the analysis. This was corroborated by numerical comparisons to the also developed redundancy test, which is based on the fundamental redundancy properties of mean-field solutions.¹⁵

B. Reference function method

The $\Delta H(M, \Delta M)$ -technique can be extended beyond the mean-field approximation using the interacting hysteron model directly. Although the solutions of a general hysteron model with exchange and dipolar interactions have not been found so far, we successfully developed a numerical approach which is convenient for extending the method.¹² Specifically, the interacting hysteron model was used to compute “reference” $\Delta H(M, \Delta M)$ data, F_{ref} , for different exchange and dipolar interaction strengths, standard deviation $\sigma = 1$, and variable $\tilde{\sigma}$ to obtain different asymmetries γ of the SFD.

Then using a general property of the hysteron model that the hysteresis data for a given asymmetry depend only on the ratios $H_{\text{ex}}/\sigma, H_{\text{dp}}/\sigma, H/\sigma$ and not on the four quantities separately,^{15,18} the field-differences corresponding to SFDs with different σ (but the same asymmetry) can be related as follows:

$$\Delta H(M, \Delta M; H_{\text{EX}}, H_{\text{DP}}, \sigma, \tilde{\sigma}) = \sigma F_{\text{ref}}(M, \Delta M; H_{\text{EX}}, H_{\text{DP}}, \tilde{\sigma}), \quad (9)$$

where H_{DP} is the dipolar field strength per particle and equals to $a^{-3}VM_S$ defined in Sec. II. The reference function method is then applied by comparing the input data to all reference functions F_{ref} computed for different interaction pairs and asymmetry factors $\tilde{\sigma}$, and for each comparison obtaining the standard deviation in (9) as a fit parameter. The value of σ , which corresponds to the best fit from among all of the reference functions, is then taken as the best guess for σ and will be called σ_{fit} . The method was demonstrated to produce very accurate values $\sigma_{\text{fit}} = \sigma$ if thermal activation is absent.¹² On the other hand, even if thermal relaxation effects are present, one expects the analysis to give $\sigma_{\text{fit}} \approx \sigma$ if the method is still applicable. The method is validated in this reference in the next section.

V. DATA ANALYSIS AND DISCUSSION

To study the accuracy of the $\Delta H(M, \Delta M)$ -method, we used the SW model defined in Sec. II to compute room temperature hysteresis data, including recoil curves, for a system of $N = 160 \times 160$ particles with $V = 4 \times 10^2 \text{ nm}^3$ and $H_K \approx 26.6 \text{ kOe}$. This gives the thermal stability ratio $KV/k_B T \approx 77.7$, which is relevant for magnetic recording. The exchange field constant H_{EX} was varied in the range 0–20 kOe, the sweep rate r from 5×10^{-2} to $5 \times 10^9 \text{ Oe/s}$, and situations with dipolar interactions turned on and off were investigated.

Figure 3 shows the computed $\Delta H(M, \Delta M)$ data extracted based on 4 recoil curves, which were computed assuming $M_S = 600 \text{ emu/cm}^3$, uniform volume ($\sigma_V = 0$, Fig. 1), and $\sigma_K \approx 20\% H_K = 5.3 \text{ kOe}$. Figures 3(a) and 3(c) correspond to the exchange field $H_{\text{EX}} = 4 \text{ kOe}$ and field sweep rates $r_1 = 5 \times 10^9 \text{ Oe/s}$ and $r_2 = 5 \times 10^{-2} \text{ Oe/s}$, respectively. The main difference is the reduction in the ΔH values for r_2 , which is a manifestation of the fact that the hysteresis loop becomes narrower for more pronounced thermal relaxation effects. In both cases we find the fit of the mean-field formula (8) (full line) as well as the reference function $\Delta H(M, \Delta M)$ -method (dashed line) to agree very well with the computed data and both methods give correct fit values $\sigma_{\text{fit}} \approx \sigma$. The situation is different for an increased exchange field $H_{\text{EX}} = 10 \text{ kOe}$ shown in Figs. 3(b) and 3(d). In this case, deformation of the $\Delta H(M, \Delta M)$ data sets near the low magnetization end, resulting from strong exchange, can no longer be described by the mean field approximation. As a result the best fit of the mean-field formula (8) does not reproduce the input data accurately. In both cases r_1 and r_2 we found the mean-field fit parameter σ_{fit} to deviate by about 30% from σ . On the other hand, as can be seen from the figures, the reference function $\Delta H(M, \Delta M)$ -method is capable of describing

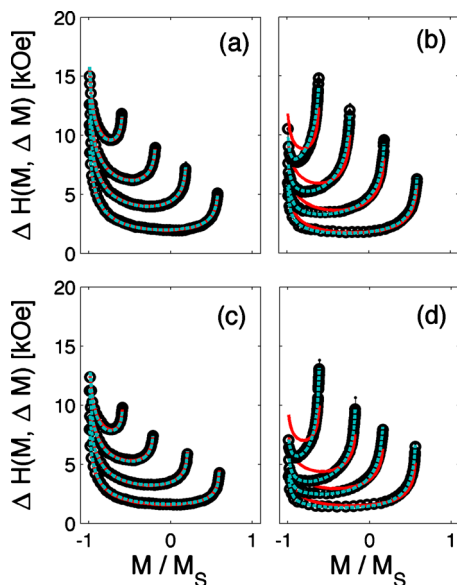


FIG. 3. (Color online) Fit of the mean-field formula, Eq. (8), (solid line) and the reference $\Delta H(M, \Delta M)$ -method, Eq. (9), (dashed line) to $\Delta H(M, \Delta M)$ data computed from the SW model with thermal excitation (circles) for parameters $M_S = 600$ emu/cm³ (in all cases) and exchange fields and external field sweep rates: (a) $H_{EX} = 4$ kOe and $r = 5 \times 10^9$ Oe/s, (b) $H_{EX} = 10$ kOe and $r = 5 \times 10^9$ Oe/s, (c) $H_{EX} = 4$ kOe and $r = 5 \times 10^{-2}$ Oe/s, and (d) $H_{EX} = 10$ kOe and $r = 5 \times 10^{-2}$ Oe/s.

the SW data surprisingly well even for the pronounced thermal relaxation cases for low r , and for all rates we recovered correct values $\sigma_{fit} \approx \sigma$. This seems rather surprising especially because the reference function method has been developed based on the nonthermal interacting hysteron model which ignores any possibility of thermal activation.

To illustrate our overall findings, Fig. 4(a) shows the

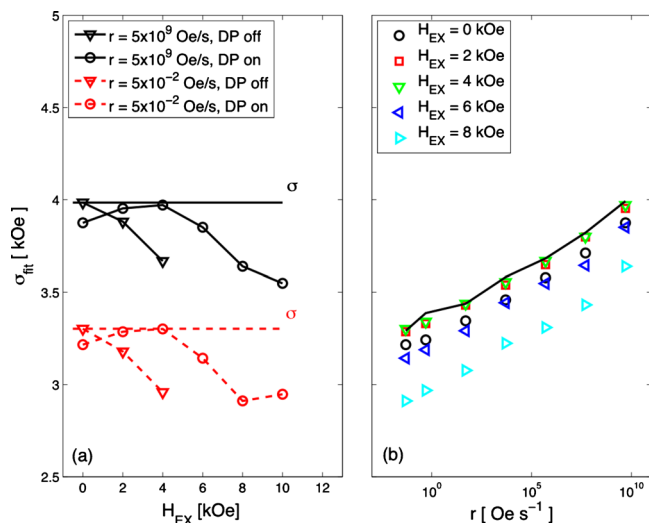


FIG. 4. (Color online) (a) σ_{fit} obtained using the mean-field $\Delta H(M, \Delta M)$ -method as a function of exchange fields H_{EX} for fast and slow external field rates r computed from the SW model using $M_S = 600$ emu/cm³, $\sigma_V = 0\%V$, and dipolar interactions turned on and off. The straight lines correspond to the correct “intrinsic” σ at the respective field sweep rates r . (b) Dependence of σ_{fit} on the field sweep rate r for different exchange fields H_{EX} . The solid line represents the “intrinsic” σ . For every r , σ was calculated directly from the derivative of the noninteracting case major hysteresis loop. Errorbars are consistently below 3% of the nominal values.

dependence of σ_{fit} vs. H_{EX} extracted using the mean-field $\Delta H(M, \Delta M)$ -method for dipolar fields turned on (circles) and off (triangles), and field sweep rates $r_1 = 5 \times 10^9$ Oe/s (solid line) and $r_2 = 5 \times 10^{-2}$ Oe/s (dashed line). The horizontal lines correspond to the correct value of the SFD’s standard deviation σ , and were obtained by a direct differentiation of the noninteracting case major hysteresis loop as discussed in Sec. III. For high rate r_1 (when thermal relaxation is essentially irrelevant) and dipolar interactions turned on, we find the highest accuracy of the method for exchange field $H_{EX} \approx 4.0$ kOe. Indeed, at these specific numerical values, the exchange field nearly compensates the dipolar fields caused by immediate neighbors making the mean-field approximation highly accurate. This behavior, resulting from ‘compensation of immediate-neighbor interactions’, has been discussed previously within the context of the nonthermal interacting hysteron model.¹⁵ When the dipolar interaction is turned off, the exchange interaction cannot be compensated and as a result, as can be seen also from the figure, the method is most accurate at $H_{EX} = 0$, i.e., for the trivial noninteracting particle system.

Similar behavior is seen for the reduced field sweep rate r_2 . In this case, σ values are smaller due to more pronounced thermal relaxation. Although the SFD shrinks, interestingly, the interaction compensation point where the method is accurate remains the same as previously. This behavior is confirmed further in Fig. 4(b), which shows the dependence of σ_{fit} on the field sweep rate r for different H_{EX} and the dipolar interactions turned on. The solid line corresponds to “intrinsic” σ obtained for the noninteracting case. The best agreement between σ and σ_{fit} is found for $H_{EX} \approx 4.0$ kOe consistently for all field sweep rates r . This suggests that within the assumed modeling picture the interaction compensation point is independent of the amount of thermal relaxation.

Application of the reference function $\Delta H(M, \Delta M)$ -method to the same set of the SW-model data is shown in Fig. 5. We find that all identified data points fall on top of the noninteracting case line accurately yielding $\sigma_{fit} \approx \sigma$ in the entire range of interactions up to $H_{EX} = 10$ kOe. In Fig. 6 we further verified the capability of the reference function $\Delta H(M, \Delta M)$ -method to extract the SFD accurately in the presence of interactions by applying it to additional data computed from the SW-model for cases $M_S = 600$ emu/cm³ and 400 emu/cm³, and considering also volume distributions with $\sigma_V = 0\%V$, $\sigma_V = 11\%V$, and $22\%V$ (Fig. 1). It is found in all cases that the interacting particle system data again agree well with the noninteracting case and also with the SFD width σ obtained by a direct differentiation of the noninteracting case major hysteresis loop, further demonstrating the ability of the $\Delta H(M, \Delta M)$ -method to extract the SFD in the presence of interparticle interactions and grain volume distributions. As can also be seen from Fig. 6, the grain size dispersion further broadens the SFD. This effect is particularly visible for slow rates with more pronounced thermal relaxation. This essentially reflects the fact that the presence of grain size distribution further contributes to the dispersion of thermally activated switching processes of par-

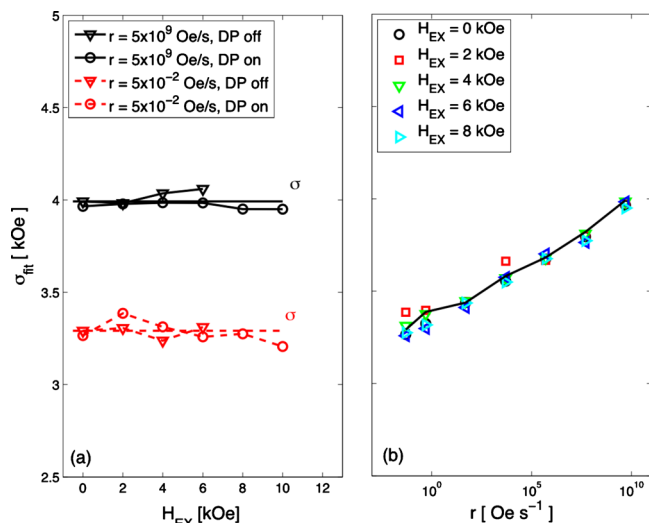


FIG. 5. (Color online) (a) σ_{fit} obtained using the reference function $\Delta H(M, \Delta M)$ -method as a function of exchange fields H_{EX} for fast and slow external field rates r computed from the SW model using $M_S = 600$ emu/cm 3 , $\sigma_V = 0\%$, and dipolar interactions turned on and off. The straight lines correspond to the correct "intrinsic" σ at the respective field sweep rates r . (b) Dependence of σ_{fit} on the field sweep rate for different exchange fields H_{EX} . The solid line represents the "intrinsic" σ . For every r , σ was calculated directly from the derivative of the noninteracting case major hysteresis loop. Errorbars are consistently below 3% of the nominal values.

ticles. Yet, it does not compromise the ability of the $\Delta H(M, \Delta M)$ -method to measure grain level properties, even in the presence of large interactions.

For very strong exchange interaction with $H_{\text{EX}} > 10$ kOe, however, even the reference function $\Delta H(M, \Delta M)$ -method shows reduced accuracy. Generally, the present modeling framework allows for two physically different mechanisms, relevant either individually or simultaneously, which may lead to this failure of the method. First, the interaction fields may become sufficiently strong in comparison to the anisotropy fields H_K and increase the possibility of noncollinear magnetization reversal and reversible magnetization processes. This scenario cannot be captured by any characterization methodology based on the hysteron picture, which ignores reversible magnetization switching. Second, if the exchange interactions dominate all other energy terms, they induce fully correlated magnetization reversal, at which point identification of any kind of microscopic information from hysteresis loops becomes impossible.¹² In the present cases for $M_S = 600$ and 400 emu/cm 3 and high exchange we attribute the reduction of the accuracy to the increasing relevance of both mechanisms. However, if the dipolar interactions are turned off, the mechanism of fully correlated reversal occurs at around $H_{\text{EX}} \approx 12$ kOe for $r_1 = 5 \times 10^9$ Oe/s, decreasing to $H_{\text{EX}} \approx 6$ kOe at $r_2 = 5 \times 10^{-2}$ Oe/s due to the narrowing of the SFD.

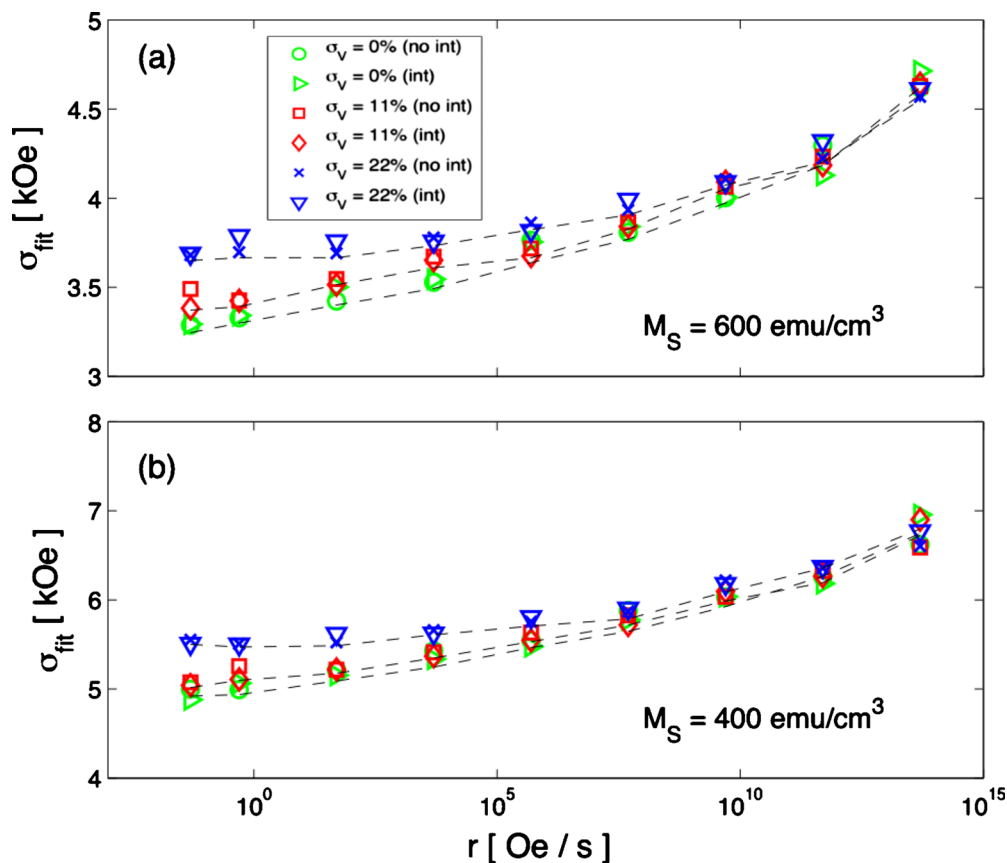


FIG. 6. (Color online) σ_{fit} obtained using the reference function $\Delta H(M, \Delta M)$ -method for different external field sweep rates r computed from the SW model for three grain size distribution widths σ_V (Fig. 1) and (a) $M_S = 600$ emu/cm 3 and (b) $M_S = 400$ emu/cm 3 . For every σ_V shown are data for the interacting case with dipolar interactions and exchange $H_{\text{EX}} = 4$ kOe (int) and noninteracting case with all interactions turned off (no int). Dashed lines correspond to the correct "intrinsic" σ at the respective field sweep rates r determined by differentiating the noninteracting case major hysteresis loop (Sec. III). Errorbars are consistently below 3% of the nominal values.

Finally, it is worthwhile to highlight the fact, that the reference function $\Delta H(M, \Delta M)$ -method is capable of recovering the correct “intrinsic” standard deviation σ of the SFD independently of interactions and even if grain size dispersion is included in the modeling. This can be attributed to the fact that (1) in the parameter range considered here, which is guided by the properties of perpendicular recording media, the interacting hysteron model represents the highly aligned SW particle system well and (2) that in the present implementation of the SW-model the evaluation of energy barriers ignores possible collective reorientations of neighboring particles during the reversal process, i.e., uses an effective field single-particle approach. The discussion of the role of this approximation in terms of the overall behavior of magnetization reversal is outside of scope of the present work and will be subject of future investigations.

VI. CONCLUSIONS

In the present work, the accuracy of the mean-field and reference function $\Delta H(M, \Delta M)$ -methods was tested by analyzing the hysteresis data computed from an interacting SW particle model of perpendicular recording materials, which included the anisotropy field and grain size distributions. The model also allows for the introduction of thermal relaxation by setting the rate of the external field variation and is suitable for investigating the relationship between the SFDs extracted from hysteresis loops at different measurement time scales. The mean-field $\Delta H(M, \Delta M)$ -method was found accurate only for comparable strengths of magnetostatic and exchange interparticle interactions. The reference function $\Delta H(M, \Delta M)$ -method, on the other hand, gave accurate results in a wide range of interactions, which includes realistic perpendicular recording materials. Our results indicate that the $\Delta H(M, \Delta M)$ -method is an accurate tool for studying thermal relaxation effects on the SFD in general interacting particle systems including the ones, in which anisotropy¹⁹ and grain size dispersion are present.

ACKNOWLEDGMENTS

Work at nanoGUNE acknowledges the EROTEK Program, Project No. IE06-172, and the Spanish Ministry of Science and Education under the Consolider-Ingenio 2010 Program, Project No. CSD2006-53. O.H. acknowledges the Marie Curie International Reintegration Grant, Project No. 224924.

- ¹S. N. Piramanayagam and K. Srinivasan, *J. Magn. Magn. Mater.* **321**, 485 (2009).
- ²H. J. Richter and S. D. Harkness, *MRS Bull.* **31**, 384 (2006).
- ³D. Weller and A. Moser, *IEEE Trans. Magn.* **35**, 4423 (1999).
- ⁴C. R. Pike, A. P. Roberts, and K. L. Verosub, *J. Appl. Phys.* **85**, 6660 (1999).
- ⁵M. Winklhofer and G. T. Zimanyi, *J. Appl. Phys.* **99**, 08E710 (2006).
- ⁶R. J. M. van de Veerdonk, X. Wu, and D. Weller, *IEEE Trans. Magn.* **39**, 590 (2003).
- ⁷I. Tagawa and Y. Nakamura, *IEEE Trans. Magn.* **27**, 4975 (1991).
- ⁸A. Berger, Y. H. Xu, B. Lengsfeld, Y. Ikeda, and E. E. Fullerton, *IEEE Trans. Magn.* **41**, 3178 (2005).
- ⁹A. Berger, B. Lengsfeld, and Y. Ikeda, *J. Appl. Phys.* **99**, 08E705 (2006).
- ¹⁰T. Shimatsu, T. Kondo, K. Mitsuzuka, S. Watanabe, H. Aoi, H. Muraoka, and Y. Nakamura, *IEEE Trans. Magn.* **43**, 2091 (2007).
- ¹¹T. Shimatsu, T. Kondo, K. Mitsuzuka, S. Watanabe, H. Aoi, H. Muraoka, and Y. Nakamura, *J. Appl. Phys.* **99**, 08F905 (2006).
- ¹²O. Hovorka, Y. Liu, K. A. Dahmen, and A. Berger, *J. Magn. Magn. Mater.* **322**, 459 (2010).
- ¹³O. Hovorka, Y. Liu, K. A. Dahmen, and A. Berger, *Appl. Phys. Lett.* **95**, 192504 (2009).
- ¹⁴R. W. Chantrell, N. Walmsley, J. Gore, and M. Maylin, *Phys. Rev. B* **63**, 024410 (2000).
- ¹⁵Y. Liu, K. A. Dahmen, and A. Berger, *Appl. Phys. Lett.* **92**, 222503 (2008).
- ¹⁶G. Bertotti, *Hysteresis in Magnetism: For Physicists, Material Scientists, and Engineers* (Academic, New York, 1998), p. 227.
- ¹⁷Y. Liu, K. A. Dahmen, and A. Berger, *Phys. Rev. B* **77**, 054422 (2008).
- ¹⁸J. P. Sethna, K. A. Dahmen, and O. Perkovic, in *The Science of Hysteresis II*, edited by G. Bertotti and I. Mayergoyz (Academic, New York, 2006), pp. 107–179.
- ¹⁹O. Hovorka, R.F. L. Evans, R.W. Chantrell, and A. Berger, *Appl. Phys. Lett.* **97**, 062504 (2010).